Performance Analysis of MIMO-OTFS with Selective Decode and Forward Relaying

Vighnesh S Bhat and A. Chockalingam
Department of ECE, Indian Institute of Science, Bangalore 560012

2023 IEEE 98th Vehicular Technology Conference (VTC2023-Fall) | 979-8-3503-2928-5/23/$31.00 ©2023 IEEE | DOI: 10.1109/VTC2023-Fall60731.2023.10333345

***Abstract*—In this paper, we analyze the performance of multiple-input multiple-output orthogonal time frequency space (MIMO-OTFS) modulation with selective decode-and-forward (SDaF) relaying. Communication between the sender and destination nodes happens in two hops using multiple relays out of which some selected relays aid the communication. All the nodes are provided with multiple transmit and multiple receive antennas. We derive closed-form expressions for the end-to-end pairwise error probability and bit error probability upper bounds in MIMO-OTFS with SDaF relaying, and characterize the achieved asymptotic diversity orders. We also investigate the considered system when phase rotation of OTFS frames is performed to improve the diversity performance. Simulation results are shown to validate the analytically predicted diversity results.**

***Index Terms*—OTFS modulation, MIMO-OTFS, selective decode-and-forward relaying, pairwise error probability, diversity analysis.**

I. Introduction

As carrier frequencies increase and high-speed use cases emerge in next generation mobile communications, modulation waveforms have to deal with high-Doppler channels which are rapidly time-varying. Orthogonal time frequency space (OTFS) modulation has been shown to offer robust performance in high-Doppler channels [1]. OTFS modulation multiplexes information symbols in the delay-Doppler (DD) domain. Several papers in the literature have examined various aspects in OTFS, such as low-complexity signal detection, DD channel estimation, peak-to-average power ratio, pulse shaping, and multiple access [2]-[4]. In terms of performance analysis of OTFS, the work reported in [5] analyzed the diversity performance of OTFS in a point-to-point setting. This study showed that the asymptotic diversity order achieved by uncoded single-input single-output OTFS is one. Also, it demonstrated that full diversity in the DD domain is achieved when phase rotation is applied to the OTFS signal vector before transmission. Results on the achievable diversity orders in both spatial and DD domains have been reported for multiple-input multiple-output OTFS (MIMO-OTFS) and space-time coded OTFS (STC-OTFS) in [5] and [6], respectively. In [6], the performance of different multi-antenna OTFS systems with receive antenna selection are analyzed and the achievable diversity orders are derived. The error performance of coded OTFS is analyzed in [7], which shows a trade-off between the coding gain and the diversity gain in OTFS systems. The bit error rate (BER) performance of OTFS with zero-forcing receiver is analyzed in [8].

Cooperative relaying is a widely recognized means to enhance the range and coverage in wireless communications [9], [10]. Amplify-and-forward and decode-and-forward protocols are widely studied owing to their simplicity and practicality. Single-relay and multi-relay schemes without and with relay selection have been investigated in a variety of system settings [11]-[13]. The performance of cooperative communication in the presence of node mobility has been studied in [13], where it has been shown that node mobility causes performance degradation. The inherent robustness of OTFS can alleviate this issue in cooperative communications with node mobility. Therefore, understanding the performance of OTFS in relaying systems in high-mobility environments is of interest. In this paper, we present an analysis of the end-to-end performance of MIMO-OTFS in selective decode-and-forward (SDaF) relaying systems. Our contributions in this paper are as follows.

- We derive closed-form expressions for the end-to-end pairwise error probability (PEP) and bit error probability upper bounds for MIMO-OTFS with SDaF relaying, and characterize the achieved asymptotic diversity orders.
- We also analyze the system when phase rotation (PR) of OTFS frames is employed to achieve improved diversity performance.
- Simulation results are shown to corroborate the analytically derived diversity orders for MIMO-OTFS with SDaF relaying.

The remainder of the paper is organized as follows. The considered OTFS system model with SDaF relaying is presented in Sec. II. The performance analysis of this system is presented in Sec. II-B. Numerical results and discussions are presented in Sec. III. A summary of conclusions is given in Sec. IV.

Notations: A matrix is denoted by uppercase boldface letter, a vector by lowercase boldface letter, a diagonal matrix with entries $x_1, \cdots, x_n$ by diag$\{x_1, \cdots, x_n\}$, and Frobenius norm of matrix $\mathbf{X}$ by $\|\mathbf{X}\|$. $(\cdot)^T$, $(\cdot)^H$, $(\cdot)^*$ denote transposition, Hermitian, and conjugation operators, respectively. A complex Gaussian distribution with mean a and variance b is denoted by $\mathcal{CN}(a, b)$. Expectation operation is denoted by $\mathbb{E}[\cdot]$. $|.|$ denotes absolute value of a number or cardinality of a set.

II. System model

The OTFS modulation and demodulation consist of 2D transforms at the transmitter and the receiver. MN information symbols, $y[k, l]$, $k = 0, \cdots, N-1$, $l = 0, \cdots, M-1$, are multiplexed over a $N \times M$ DD grid, given by $\{(\frac{k}{NT}, \frac{l}{M\Delta f}), k = 0, \cdots, N-1, l = 0, \cdots, M-1\}$, where M and N are the number of delay and Doppler bins, respectively, and $\frac{1}{M\Delta f}$ and $\frac{1}{NT}$ are the delay and Doppler bin sizes, respectively. The information symbols in the DD domain are mapped to the

This work was supported by the J. C. Bose National Fellowship, Department of Science and Technology, Government of India.

TF domain using inverse symplectic finite Fourier transform (ISFFT) and windowing. The TF symbols are converted to time domain using Heisenberg transform for transmission over the channel. At the receiver, the time domain signal is converted to TF domain using Wigner transform, which is converted to DD domain using SFFT. The end-to-end input-output relation in the DD domain is given by [3]

$$z[k,l] = \sum_{i=1}^{P} g_i' y[(k-\beta_i)_N, (l-\alpha_i)_M] + v[k,l], \quad (1)$$

where $g_i' = g_i e^{-j2\pi\nu_i\tau_i}$, (g_i, τ_i, ν_i) are the channel coefficient, delay, and Doppler of the ith path, respectively, P is the number of paths, g_is are i.i.d and distributed as $\mathcal{CN}(0, 1/P)$ with uniform scattering profile, α_i and β_i are integers corresponding to indices of delay and Doppler, respectively, for the ith path, i.e., $\tau_i \triangleq \frac{\alpha_i}{M\Delta f}$ and $\nu_i \triangleq \frac{\beta_i}{NT}$, and $v[k,l]$ is the additive white Gaussian noise. By vectorizing the input-output relation in (1), we can write [3]

$$\mathbf{z} = \mathbf{G}\mathbf{y} + \mathbf{v}, \quad (2)$$

where $\mathbf{y}, \mathbf{z}, \mathbf{v} \in \mathbb{C}^{MN\times 1}$, the $(k+Nl)$th entry of $\mathbf{y}$, $y_{k+Nl} = y[k,l]$, $k = 0, \cdots, N-1$, $l = 0, \cdots, M-1$ and $y[k,l] \in \mathbb{A}$, where $\mathbb{A}$ is the modulation alphabet (e.g., QAM/PSK). Similarly, $z_{k+Nl} = z[k,l]$ and $v_{k+Nl} = v[k,l]$, $k = 0, \cdots, N-1, l = 0, \cdots, M-1$, and $\mathbf{G} \in \mathbb{C}^{MN\times MN}$ is the effective channel matrix, whose jth row ($j = k + Nl$), denoted by $\mathbf{G}[j]$, is given by $\mathbf{G}[j] = [\hat{g}((k-0)_N, (l-0)_M) \;\; \hat{g}((k-1)_N, (l-0)_M) \;\; \cdots \hat{g}((k-N-1)_N, (l-M-1)_M)]$, where $\hat{g}(k,l)$ denotes the (k,l)th element of the $N \times M$ DD channel matrix, given by

$$\hat{g}(k,l) = \begin{cases} g_i' & \text{if } k = \beta_i,\ l = \alpha_i,\ i \in \{1, 2, \cdots, P\} \\ 0 & \text{otherwise.} \end{cases} \quad (3)$$

It can be seen from the above that the effective channel matrix $\mathbf{G}$ has only P non-zero entries in each row and column, i.e., there are only MNP non-zero elements in $\mathbf{G}$.

An alternate representation of input-output relation (2): In order to enable the diversity analysis, the input-output relation in (2) is written in an alternate form. Observing that the effective channel matrix $\mathbf{G}$ contains only P non-zero entries in each row and column, the vectorized input-output relation in (2) can be written in the following alternate form:

$$\mathbf{z}^T = \mathbf{g}'\mathbf{Y} + \mathbf{v}^T, \quad (4)$$

where $\mathbf{g}' \in \mathbb{C}^{1\times P}$ is the channel vector with ith entry given by $g_i' = g_i e^{-j2\pi\nu_i\tau_i}$, $\mathbf{z}^T$, $\mathbf{v}^T \in \mathbb{C}^{1\times MN}$, are the received signal vector and noise vector, respectively, and $\mathbf{Y} \in \mathbb{C}^{P\times MN}$ is the signal matrix with ith column $\mathbf{Y}[i]$, $i = k + Nl$, $k = 0, \cdots, N-1$, $l = 0, \cdots, M-1$, given by

$$\mathbf{Y}[i] = \begin{bmatrix} y_{(k-\beta_1)_N + N(l-\alpha_1)_M} \\ y_{(k-\beta_2)_N + N(l-\alpha_2)_M} \\ \vdots \\ y_{(k-\beta_P)_N + N(l-\alpha_P)_M} \end{bmatrix}. \quad (5)$$

A. MIMO-OTFS

The input-output relation in a MIMO-OTFS system with n_r receive antennas and n_t transmit antennas can be written as

$$\mathbf{z}_i = \sum_{j=1}^{n_t} \mathbf{G}_{ij}\mathbf{y}_j + \mathbf{v}_i, \quad i = 1, \cdots, n_r, \quad (6)$$

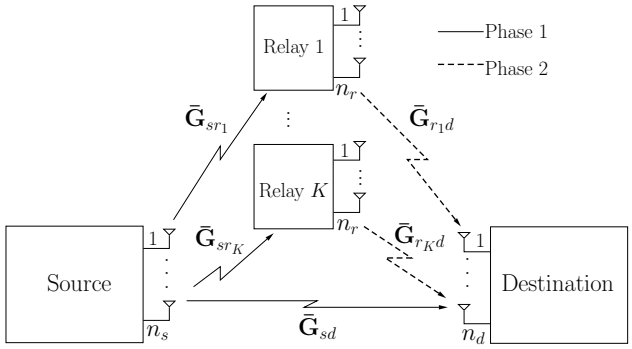

Fig. 1: MIMO-OTFS with SDaF relaying.

where $\mathbf{G}_{ij}$ is the effective channel matrix between the jth transmit and ith receive antennas. Concatenating $\mathbf{z}_i$, (6) can be written as

$$\bar{\mathbf{z}} = \bar{\mathbf{G}}\bar{\mathbf{y}} + \bar{\mathbf{v}}, \quad (7)$$

where $\bar{\mathbf{z}} = [\mathbf{z}_1^T, \ \mathbf{z}_2^T, \cdots \mathbf{z}_{n_r}^T]^T \in \mathbb{C}^{n_r MN\times 1}$, $\mathbf{z}_i$ being the received signal vector of the ith receive antenna, $\bar{\mathbf{y}} = [\mathbf{y}_1^T, \ \mathbf{y}_2^T, \cdots, \ \mathbf{y}_{n_t}^T]^T \in \mathbb{C}^{n_t MN\times 1}$, $\mathbf{y}_j$ being the transmit signal vector from the jth transmit antenna, $\bar{\mathbf{v}} = [\mathbf{v}_1^T, \ \mathbf{v}_2^T, \cdots, \ \mathbf{v}_{n_r}^T]^T \in \mathbb{C}^{n_r MN\times 1}$, $\mathbf{v}_i$ being the noise vector of the ith receive antenna, and $\bar{\mathbf{G}} \in \mathbb{C}^{n_r MN\times n_t MN}$ is the overall effective MIMO-OTFS channel matrix.

An alternate input-output relation for MIMO-OTFS: We observe that in the overall effective MIMO-OTFS channel matrix $\bar{\mathbf{G}}$, each row contains only $n_t P$ unique non-zero elements and each column contains $n_r P$ unique non-zero elements. Therefore, (7) can be written in the following alternate form:

$$\mathbf{z}_i^T = \sum_{j=1}^{n_t} \mathbf{g}_{ij}'\mathbf{Y}_j + \mathbf{v}_i^T, \quad i = 1, \cdots, n_r, \quad (8)$$

Concatenating $\mathbf{z}_i^T$, (8) can be written in a compact form as

$$\tilde{\mathbf{Z}} = \tilde{\mathbf{G}}\tilde{\mathbf{Y}} + \tilde{\mathbf{V}}, \quad (9)$$

where $\tilde{\mathbf{Z}} \in \mathbb{C}^{n_r\times MN}$ is the received signal matrix with $\mathbf{z}_i^T$ as the row corresponding to the ith receive antenna, $\tilde{\mathbf{G}} \in \mathbb{C}^{n_r\times n_t P}$ is the channel matrix with $\mathbf{g}_{ij}' \in \mathbb{C}^{1\times P}$ being the row containing the unique non-zero entries of the channel matrix $\mathbf{G}_{ij}$, $\tilde{\mathbf{Y}} \in \mathbb{C}^{n_t P\times MN}$ is the transmit symbol matrix with $\mathbf{Y}_j \in \mathbb{C}^{P\times MN}$ being the transmit signal matrix from the jth transmit antenna, and $\tilde{\mathbf{V}} \in \mathbb{C}^{n_r\times MN}$ is the noise matrix.

B. Selective decode and forward relaying

The considered selective decode and forward relaying scheme is presented here. Figure 1 shows the block diagram of the MIMO-OTFS scheme with SDaF relaying. In this scheme, in addition to a direct link, there are K relays between the source and destination to aid the communication. Let n_s and n_r denote the number of transmit antennas at the source (S) and relay (R), respectively, and n_d denote the number of receive antennas at the destination (D), $n_d \geq n_r = n_s$. In sDaF relaying, the source transmits the message to the destination and relays during the first phase. In the first phase, the destination will not decode the message, but all the relays will decode the message. The relays that decode the message correctly will forward the decoded message to the destination

in the second phase. In the second phase, the destination *jointly* decodes the messages received from the source (in the first phase) and the forwarding relays (in the second phase).

In the first phase, the received signal at the kth relay, $k = 1, 2, \cdots, K$, and the destination are given by

$$\bar{\mathbf{z}}_{sr_k} = \bar{\mathbf{G}}_{sr_k}\bar{\mathbf{y}} + \bar{\mathbf{v}}_{sr_k}, \tag{10}$$

$$\bar{\mathbf{z}}_{sd} = \bar{\mathbf{G}}_{sd}\bar{\mathbf{y}} + \bar{\mathbf{v}}_{sd}, \tag{11}$$

where $\bar{\mathbf{z}}_{sr_k} \in \mathbb{C}^{n_r MN\times 1}$, $\bar{\mathbf{z}}_{sd} \in \mathbb{C}^{n_d MN\times 1}$ are the received signal vectors at the kth relay (R_k) and destination, respectively, $\bar{\mathbf{G}}_{sr_k} \in \mathbb{C}^{n_r MN\times n_s MN}$, $\bar{\mathbf{G}}_{sd} \in \mathbb{C}^{n_d MN\times n_s MN}$ are the effective channel matrices between S-to-R_k, and S-to-D, respectively, $\bar{\mathbf{y}} \in \mathbb{C}^{n_s MN\times 1}$ is the transmit signal vector, and $\bar{\mathbf{v}}_{sr_k} \in \mathbb{C}^{n_r MN\times 1}$, $\bar{\mathbf{v}}_{sd} \in \mathbb{C}^{n_d MN\times 1}$ are the noise vectors at R_k and D, respectively. In the second phase, the relays transmit one-by-one in K orthogonal time slots [12]. Let Ω denote the set of relays which decoded the message correctly. The received signal at the destination on the R_k-to-D link is then given by

$$\bar{\mathbf{z}}_{r_k d} = \bar{\mathbf{G}}_{r_k d}\bar{\mathbf{y}} + \bar{\mathbf{v}}_{r_k d}, \quad \forall k \in \Omega, \tag{12}$$

where $\bar{\mathbf{z}}_{r_k d}, \bar{\mathbf{v}}_{r_k d} \in \mathbb{C}^{n_d MN\times 1}$ are the received signal and noise vectors, respectively, for the R_k-to-D link, $\bar{\mathbf{G}}_{r_k d} \in \mathbb{C}^{n_d MN\times n_r MN}$ is the effective channel matrix on the R_k-to-D link, and $\bar{\mathbf{y}} \in \mathbb{C}^{n_r MN\times 1}$ is the transmit signal vector.

Alternate form for MIMO-OTFS with SDaF: The input-output relation in (10), (11), and (12) can be written in an alternate form as follows. The received signals at R_k and D in the first phase are

$$\tilde{\mathbf{Z}}_{sr_k} = \tilde{\mathbf{G}}_{sr_k}\tilde{\mathbf{Y}} + \tilde{\mathbf{V}}_{sr_k}, \quad k = 1, 2, \cdots, K, \tag{13}$$

$$\tilde{\mathbf{Z}}_{sd} = \tilde{\mathbf{G}}_{sd}\tilde{\mathbf{Y}} + \tilde{\mathbf{V}}_{sd}, \tag{14}$$

where $\tilde{\mathbf{Z}}_{sr_k}, \tilde{\mathbf{V}}_{sr_k} \in \mathbb{C}^{n_r\times MN}$, $\tilde{\mathbf{Z}}_{sd}, \tilde{\mathbf{V}}_{sd} \in \mathbb{C}^{n_d\times MN}$, $\tilde{\mathbf{G}}_{sr_k} \in \mathbb{C}^{n_r\times n_s P_{sr_k}}$, and $\tilde{\mathbf{G}}_{sd} \in \mathbb{C}^{n_d\times n_s P_{sd}}$. The received signal at D on the R_k-to-D link in the second phase is given by

$$\tilde{\mathbf{Z}}_{r_k d} = \tilde{\mathbf{G}}_{r_k d}\tilde{\mathbf{Y}} + \tilde{\mathbf{V}}_{r_k d}, \quad \forall k \in \Omega, \tag{15}$$

where $\tilde{\mathbf{Z}}_{r_k d}, \tilde{\mathbf{V}}_{r_k d} \in \mathbb{C}^{n_d\times MN}$, $\tilde{\mathbf{G}}_{r_k d} \in \mathbb{C}^{n_d\times n_r P_{r_k d}}$, and P_{sr_k} and $P_{r_k d}$ are the number of resolvable DD domain paths between S-to-R_k and R_k-to-D links, respectively.

C. OTFS with phase rotation

Phase rotation (PR) of symbols in the OTFS signal vector can be performed before transmission in order to achieve improved DD domain diversity. PR in OTFS is performed by pre-multiplying the OTFS vector $\mathbf{y}$ by a PR matrix $\mathbf{\Theta}$, given by $\mathbf{\Theta} = \text{diag}\{e^{j\frac{q}{MN}}\}$, $q = 0, \cdots, MN-1$. Therefore, $\mathbf{y}' = \mathbf{\Theta}\mathbf{y}$ is the phase rotated OTFS transmit vector.

III. Performance analysis with SDaF relaying

In this section, we analyze the diversity performance of MIMO-OTFS with SDaF relaying. Maximum likelihood (ML) detection is considered at the relays and the destination. The minimum rank of the difference matrices in a given system plays a key role in determining the diversity performance of the system. Therefore, we first characterize the minimum rank in the considered relaying system.

A. Minimum rank on various links with relaying

In the S-to-R_k link, let $\tilde{\mathbf{Y}}_i$ and $\tilde{\mathbf{Y}}_j$ be two distinct MIMO-OTFS symbol matrices without PR defined in (13), and $\tilde{\mathbf{Y}}'_i$ and $\tilde{\mathbf{Y}}'_j$ be two such matrices with PR. As in [5], the minimum ranks of $(\tilde{\mathbf{Y}}_i - \tilde{\mathbf{Y}}_j)$ and $(\tilde{\mathbf{Y}}'_i - \tilde{\mathbf{Y}}'_j)$ on the S-to-R link for MIMO-OTFS are 1 and P_{sr_k}, respectively. Similarly, the minimum ranks of $(\tilde{\mathbf{Y}}_i - \tilde{\mathbf{Y}}_j)$ and $(\tilde{\mathbf{Y}}'_i - \tilde{\mathbf{Y}}'_j)$ on the S-to-D link for MIMO-OTFS are 1 and P_{sd}, respectively. Now, consider the R_k-to-D link. In this scheme, a given relay will forward the symbol vector in the second phase if it correctly decoded the message in the first phase. In the R_k-to-D link, let $\tilde{\mathbf{Y}}_i$ and $\tilde{\mathbf{Y}}_j$ denote two distinct symbol matrices without PR, and let $\tilde{\mathbf{Y}}'_i$ and $\tilde{\mathbf{Y}}'_j$ denote two such matrices with PR. We are interested in the minimum rank of the difference matrix $(\tilde{\mathbf{Y}}_i - \tilde{\mathbf{Y}}_j)$, $\forall i, j$. To find that, we note that the elements of the symbol matrices $\tilde{\mathbf{Y}}_i$ and $\tilde{\mathbf{Y}}_j$ are symbols from the modulation alphabet $\mathbb{A}$. Without PR, the set of all the possible symbol matrices will include the matrix $a\mathbf{1}_{n_r P_{r_k d}\times MN}$, where $a \in \mathbb{A}$. Now, considering the two distinct matrices to be $\tilde{\mathbf{Y}}_i = a\mathbf{1}_{n_r P_{r_k d}\times MN}$ and $\tilde{\mathbf{Y}}_j = a'\mathbf{1}_{n_r P_{r_k d}\times MN}$, $a \neq a'$, the difference matrix is given by $(a - a')\mathbf{1}_{n_r P_{r_k d}\times MN}$ whose all elements will be the same. Therefore, its rank is one which is the minimum rank. Next, with PR, letting $\tilde{\mathbf{\Delta}}'_{ij} = (\tilde{\mathbf{Y}}'_i - \tilde{\mathbf{Y}}'_j)$, we have

$$\tilde{\mathbf{\Delta}}'_{ij} = \begin{bmatrix} \mathbf{\Delta}'_{1,ij} \\ \vdots \\ \mathbf{\Delta}'_{n_r,ij} \end{bmatrix}, \tag{16}$$

where $\mathbf{\Delta}'_{m,ij} = \mathbf{Y}'_{m,i} - \mathbf{Y}'_{m,j}$, and $\mathbf{Y}'_{m,i}$ and $\mathbf{Y}'_{m,j}$ are the transmitted symbol matrices from the mth antenna. The minimum rank of $\mathbf{\Delta}'_{m,ij}$ is $P_{r_k d}$ for all $m = 1, \cdots, n_r$. Therefore, the minimum rank of $(\tilde{\mathbf{Y}}'_i - \tilde{\mathbf{Y}}'_j)$ is $P_{r_k d}$.

B. Diversity analysis of SDaF

As mentioned in Sec. II-B, the relays which decode the symbols successfully will forward the decoded symbols to the destination in the second phase. The K relays in the system can be in either one of two possible states depending on whether the symbols are decoded correctly or incorrectly. As a result, there are 2^K possible states. Let $a(k)$ indicate the state of the kth relay for $1 \leq k \leq K$ with $a(k) = 1$ if the kth relay decodes correctly and 0 otherwise. Let $\mathcal{S}$ denote the set which includes all possible 2^K binary states, with $\mathbf{s}_l \in \mathcal{S}$ for $0 \leq l \leq 2^K - 1$ representing one of them. The end-to-end PEP at the destination between symbol matrices $\tilde{\mathbf{Y}}_i$ and $\tilde{\mathbf{Y}}_j$ assuming $\tilde{\mathbf{Y}}_i$ is the transmitted symbol matrix is given by [11]

$$P_e(\tilde{\mathbf{Y}}_i \to \tilde{\mathbf{Y}}_j) = \sum_{\mathbf{s}_l \in \mathcal{S}} P_e(\tilde{\mathbf{Y}}_i \to \tilde{\mathbf{Y}}_j | \mathbf{a} = \mathbf{s}_l) P(\mathbf{a} = \mathbf{s}_l), \tag{17}$$

where $\mathbf{a} = [a(1)\ a(2)\ \cdots\ a(K)]^T$ denotes the the system state vector, $P_e(\tilde{\mathbf{Y}}_i \to \tilde{\mathbf{Y}}_j | \mathbf{a} = \mathbf{s}_l)$ is the end-to-end PEP when the relays are in state $\mathbf{s}_l$, and $P(\mathbf{a} = \mathbf{s}_l)$ denotes the corresponding probability of the system being in state $\mathbf{s}_l \in \mathcal{S}$. The probability that the system will be in state $\mathbf{a} = \mathbf{s}_l \in \mathcal{S}$ can be calculated as

$$P(\mathbf{a} = \mathbf{s}_l) = \prod_{k=1}^{K} P(a(k) = s_l(k)), \tag{18}$$

where $P(a(k)=s_l(k))$ corresponds to the net PEP at the kth relay, given by

$$P(a(k)=s_l(k))= \begin{cases} \rho\sum_p\sum_{q,q\neq p} d_{pq}\ P_{S\to R_k}(\tilde{\mathbf{Y}}_p\to\tilde{\mathbf{Y}}_q), & \text{if } s_l(k)=0 \\ 1-\rho\sum_p\sum_{q,q\neq p} d_{pq}\ P_{S\to R_k}(\tilde{\mathbf{Y}}_p\to\tilde{\mathbf{Y}}_q), & \text{if } s_l(k)=1, \end{cases} \tag{19}$$

where $d_{pq}=d_H(\bar{\mathbf{y}}_p,\bar{\mathbf{y}}_q)$ is the number of information bits in $\bar{\mathbf{y}}_q$ which differ from those in $\bar{\mathbf{y}}_p$, $\rho=\frac{1}{Ln_sMN\log_2|\mathbb{A}|}$, and $L=|\mathbb{A}^{n_sMN}|$. Following similar steps in [5] for the MIMO-OTFS system in point-to-point communication, the upper bound on the average PEP between the symbol matrices $\tilde{\mathbf{Y}}_p$ and $\tilde{\mathbf{Y}}_q$ for the source and kth relay is given by

$$P_{S\to R_k}(\tilde{\mathbf{Y}}_p\to\tilde{\mathbf{Y}}_q)\leq\left(\prod_{m=1}^{r_{sr_k}}\frac{1}{(1+\frac{\lambda_{sr_k}^{mpq}\gamma_{sr_k}}{4P_{sr_k}})}\right)^{n_r}, \tag{20}$$

where r_{sr_k} is the rank of $(\tilde{\mathbf{Y}}_p-\tilde{\mathbf{Y}}_q)$ on the S-to-R_k link, $\lambda_{sr_k}^{mpq}$ is the eigenvalue of $(\tilde{\mathbf{Y}}_p-\tilde{\mathbf{Y}}_q)(\tilde{\mathbf{Y}}_p-\tilde{\mathbf{Y}}_q)^H$, and γ_{sr_k} is the normalized SNR for the S-to-R_k link. The unconditional average end-to-end PEP at the destination between $\tilde{\mathbf{Y}}_i$ and $\tilde{\mathbf{Y}}_j$ is obtained as (see Appendix A for the derivation)

$$\begin{aligned} P_e(\tilde{\mathbf{Y}}_i\to\tilde{\mathbf{Y}}_j) \ \leq\ & \gamma_{sd}^{-n_dr_{sd}}D_{ij}[\gamma_{r_1d}^{-n_dr_{r_1d}}C_1^{ij}+\gamma_{sr_1}^{-n_rr_{sr_1}}C_1] \\ & [\gamma_{r_2d}^{-n_dr_{r_2d}}C_2^{ij}+\gamma_{sr_2}^{-n_rr_{sr_2}}C_2]\cdots \\ & [\gamma_{r_Kd}^{-n_dr_{r_Kd}}C_K^{ij}+\gamma_{sr_K}^{-n_rr_{sr_K}}C_K]. \end{aligned} \tag{21}$$

For equal power allocation between source and relays, we have $\gamma_{sr_k}=\gamma_{r_kd}=\gamma_{sd}=\gamma$, $k=1,\cdots,K$. Expansion in (21) contains 2^K terms. We can write

$$\begin{aligned} P_e(\tilde{\mathbf{Y}}_i\to\tilde{\mathbf{Y}}_j) \ \leq\ & \gamma^{-\sum_{k=1}^{K}n_dr_{r_kd}}D_{ij}\Big[\gamma^{-\sum_{k=1}^{K}n_dr_{r_kd}}\prod_{k=1}^{K}C_k^{ij} \\ & +\gamma^{-\sum_{k=1}^{K-1}n_dr_{r_kd}}\gamma^{-n_rr_{sr_K}}C_K\prod_{k=1}^{K-1}C_k^{ij}+ \\ & \cdots+\gamma^{-\sum_{k=1}^{K-1}n_rr_{sr_k}}\gamma^{-n_dr_{r_Kd}}C_K^{ij}\prod_{k=1}^{K-1}C_k \\ & +\gamma^{-\sum_{k=1}^{K}n_rr_{sr_k}}\prod_{k=1}^{K}C_k\Big]. \end{aligned} \tag{22}$$

At high SNRs, the minimum power of γ will dominate. Therefore, the diversity order (DO) is given by

$$\begin{aligned} DO \ =\ & n_dr_{sd}+\min\Big\{\sum_{k=1}^{K}n_dr_{r_kd},\ \sum_{k=1}^{K-1}n_dr_{r_kd}+n_rr_{sr_K}, \\ & \cdots,\sum_{k=1}^{K-1}n_rr_{sr_k}+n_dr_{r_Kd},\ \sum_{k=1}^{K}n_rr_{sr_k}\Big\}. \end{aligned} \tag{23}$$

The above expression can be equivalently written as

$$\begin{aligned} DO \ =\ & n_dr_{sd}+\min\{n_rr_{sr_1},n_dr_{r_1d}\}+\min\{n_rr_{sr_2},n_dr_{r_2d}\} \\ & +\cdots+\min\{n_rr_{sr_K},n_dr_{r_Kd}\} \\ =\ & n_dr_{sd}+\sum_{k=1}^{K}\min\{n_rr_{sr_k},n_dr_{r_kd}\}. \end{aligned} \tag{24}$$

Parameter	Value
Carrier frequency, f_c	4 GHz
Subcarrier spacing, Δf	3.75 kHz
DD profile $(\tau_i,\ \nu_i)$ for 1 DD path	$(\frac{1}{M\Delta f},\ \frac{1}{NT})$
DD profile $(\tau_i,\ \nu_i)$ for 2 DD paths, for $M=2,4,\ N=2$	$(0,0),\ (\frac{1}{M\Delta f},\ \frac{1}{NT})$
DD profile $(\tau_i,\ \nu_i)$ for 4 DD paths, for $M=2,4,\ N=2$	$(0,0),\ (0,\frac{1}{NT}),$ $(\frac{1}{M\Delta f},0),\ (\frac{1}{M\Delta f},\frac{1}{NT})$
Maximum speed	506.2 kmph
Modulation	BPSK

TABLE I: Simulation parameters.

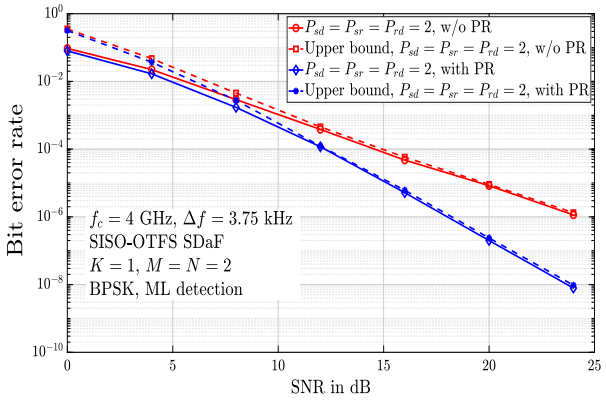

Fig. 2: BER performance of SISO-OTFS with selective DaF without and with PR for $K=1$, $P_{sd}=P_{sr}=P_{rd}=2$.

MIMO-OTFS without PR achieves a diversity of $n_d+\sum_{k=1}^{K}\min\{n_r,n_d\}=n_d+Kn_r$, since the minimum ranks are $r_{sr_k}=r_{r_kd}=r_{sd}=1$. MIMO-OTFS with PR achieves a diversity of $n_dP_{sd}+\sum_{k=1}^{K}\min\{n_rP_{sr_k},n_dP_{r_kd}\}$, since the minimum ranks are $r_{sd}=P_{sd}$, $r_{sr_k}=P_{sr_k}$, $r_{r_kd}=P_{r_kd}$.

IV. Results and Discussions

In this section, we present analytical and simulation results on the BER and diversity performance of the MIMO-OTFS scheme with SDaF relaying analyzed in the previous section. The number of DD paths considered on the various links are 1, 2, and 4. Table I shows the system parameters used in the simulations.

SISO-OTFS with SDaF relaying (without and with PR): Figure 2 shows the BER of SISO-OTFS ($n_s=n_r=n_d=1$) with selective DaF relaying without and with PR for $K=1$, $M=N=2$, $P_{sd}=2$, $P_{sr}=2$, and $P_{rd}=2$. In addition to simulated BERs, the BER upper bounds are also plotted. We observe that the upper bounds are found to be tight at high SNRs. We also observe that the diversity slope for the simulated system without PR is two and the analytically predicted diversity order in Sec. III-B is also $n_d+Kn_r=2$. The figure also shows the BER of the same system with PR. From the analysis in Sec. III-B, the achieved diversity order with PR is $P_{sd}+\min\{P_{sr},P_{rd}\}=4$. In Fig. 2, the diversity slope is observed to be 4, corroborating the analytically predicted diversity order.

MIMO-OTFS with SDaF relaying (with and without PR): Figure 3 shows the BER performance of MIMO-OTFS with

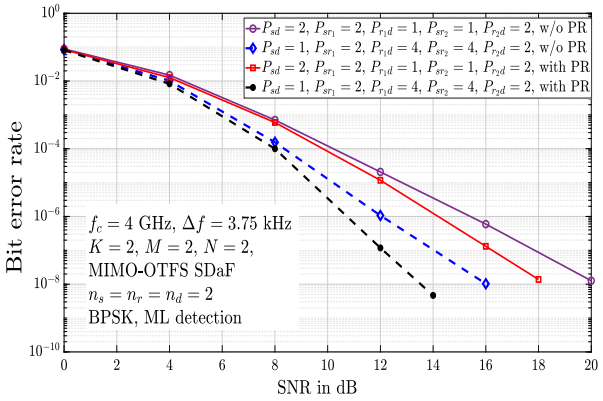

Fig. 3: BER performance of MIMO-OTFS with selective DaF without and with PR for $K=2$, $n_s=n_d=n_r=2$.

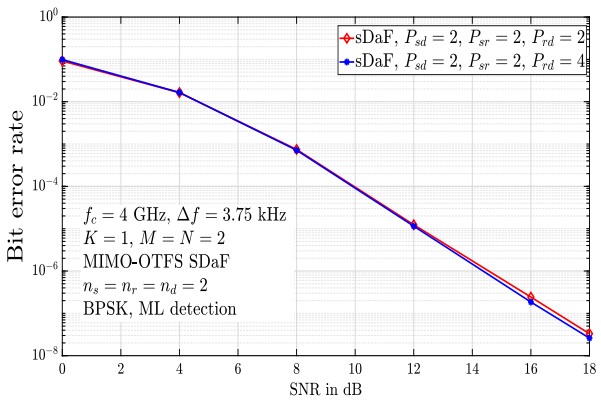

Fig. 4: BER performance of MIMO-OTFS with SDaF without PR for $M=N=2$, $n_s=n_r=n_d=2$, and fractional DDs.

selective DaF relaying with and without PR for $K=2$, $M=N=2$, $n_s=n_r=n_d=2$, $P_{sd}=1,2$, $P_{sr}=1,2,4$, and $P_{rd}=1,2,4$. From the analysis, the diversity order without PR is n_d+Kn_r. For the considered systems, these diversity orders are 6. For the system with PR, $P_{sd}=2$, $P_{sr_1}=2$, $P_{r_1d}=1$ and $P_{sr_2}=1$, $P_{r_2d}=2$, the diversity order from analysis is $n_dP_{sd}+\sum_{k=1}^{2}\min\{n_rP_{sr_k},n_dP_{r_kd}\}=4+\min\{4,2\}+\min\{2,4\}=8$. For the system with PR, $P_{sd}=1$, $P_{sr_1}=2$, $P_{r_1d}=4$ and $P_{sr_2}=4$, $P_{r_2d}=2$, the diversity order is $2+\min\{8,4\}+\min\{4,8\}=10$. The simulation BER plots indicate these high diversity slopes.

Results for fractional delay-Dopplers In Figs. 2 and 3, integer delay-Dopplers without fractional parts (as in Table I) are considered. We have carried out the performance analysis for fractional DDs also in a similar way as in Sec. III. The diversity order results are found to be the same for both fractional and integer DDs. We do not present this analysis for lack of space, and provide only the numerical results here.

Small values of (M,N)*:* Figure 4 shows the simulated BER performance of MIMO-OTFS with SDaF relaying with $K=1$ without PR for $n_s=n_r=n_d=2$, $M=N=2$, $P_{sd}=2$, $P_{sr}=2$, and $P_{rd}=2,4$. The Doppler corresponding to the ith channel tap is generated using Jakes's formula [3]. The delay corresponding to ith channel tap is generated as uniformly distributed over $[0,\frac{M-1}{M\Delta f}]$. Exponential power delay profile and Jakes Doppler spectrum are considered. ML detection is used. From Fig. 4, we observe a diversity slope of 4 for the considered MIMO-OTFS with SDaF relaying is 4, which is also the diversity order we predicted through analysis.

MIMO-OTFS vs MIMO-OFDM for large values of (M,N)*:* In Fig. 5, we compare the BER performance of MIMO-OTFS and MIMO-OFDM with SDaF relaying, utilizing system parameters according to the IEEE 802.11p standard [14]. The system operates at a carrier frequency of 5.9 GHz with a subcarrier spacing of 0.156 MHz. A frame size of $M=64$ and $N=12$ is employed for the simulations, along with $P_{sd}=P_{sr}=P_{rd}=8$ DD paths, rectangular pulse and $K=1$. Fractional DDs are used with a maximum speed of 220 km/h, corresponding to a maximum Doppler of 1.2 kHz and BPSK modulation with minimum mean square error

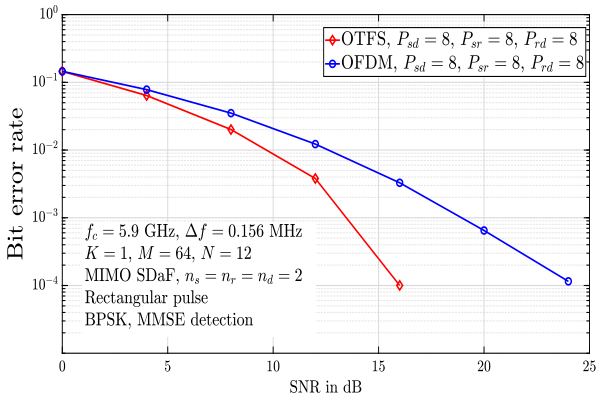

Fig. 5: BER comparison between MIMO-OTFS and MIMO-OFDM with SDaF for $M=64$, $N=12$, and fractional DDs.

(MMSE) detection is used. From Fig. 5, we observe that the performance of MIMO-OTFS is significantly better than the MIMO-OFDM system for considered relaying scheme. For example, at a BER of 10^{-3}, MIMO-OTFS with SDaF has a gain of about 6 dB compared to MIMO-OFDM with SDaF.

V. Conclusions

In this work, we investigated the performance of MIMO-OTFS systems with selective decode and forward relaying. We considered MIMO-OTFS with relaying where a selected set of relays among multiple relays aid communication between the transmitter and receiver in two hops. We derived closed-form expressions for the end-to-end PEP and BER upper bounds for this relaying system, and quantified the achieved asymptotic diversity orders with and without PR. Simulation results were shown to validate the analytically derived diversity orders. The analysis for practical pulses can be carrier out on similar lines, which can be taken as future work. Optimal power allocation schemes for the source and relay nodes and the effect of inter-node distances on the performance can also be analyzed as future work.

Appendix A
Derivation of (21)

Continuing from (20), let $\xi_l=\{k|s_l(k)=1,1\le k\le K\}$ denote the set of all relays that correctly decode the message.

The average PEP at the destination between $\tilde{\mathbf{Y}}_i$ and $\tilde{\mathbf{Y}}_j$ with relays in state $\mathbf{a} = s_l \in \mathcal{S}$ is given by

$$P_e(\tilde{\mathbf{Y}}_i \to \tilde{\mathbf{Y}}_j|\mathbf{a}=\mathbf{s}_l) \leq \prod_{m=1}^{r_{sd}} \left\{ \left(\frac{1}{1+\frac{\lambda_{sd}^{mij}\gamma_{sd}}{4P_{sd}}} \right)^{n_d} \right\} \prod_{k\in\xi_l} \prod_{m=1}^{r_{r_kd}} \left(\frac{1}{1+\frac{\lambda_{r_kd}^{mij}\gamma_{r_kd}}{4P_{r_kd}}} \right)^{n_d}, \quad (25)$$

where r_{sd} and r_{r_kd} are the ranks of $(\tilde{\mathbf{Y}}_i - \tilde{\mathbf{Y}}_j)$ on the S-to-D link and R_k-to-D link, respectively, γ_{sd} is the normalized SNR for the S-to-D link, γ_{r_kd} is the normalized SNR for the R_k-to-D link, and λ_{sd}^{mij} and $\lambda_{r_kd}^{mij}$ are the eigenvalues of $(\tilde{\mathbf{Y}}_i-\tilde{\mathbf{Y}}_j)(\tilde{\mathbf{Y}}_i-\tilde{\mathbf{Y}}_j)^H$ on the S-to-D link and R_k-to-D link, respectively. We note that at high SNRs, in (19), the term $1-\rho\sum_p\sum_{q,q\neq p} d_{pq}P_{S\to R_k}(\tilde{\mathbf{Y}}_p \to \tilde{\mathbf{Y}}_q) \approx 1$ if $s_l(k)=1$. As a result, the bound on the bit error probability for ML detection at the destination can be obtained by adding up all PEP terms corresponding to $(\tilde{\mathbf{Y}}_i \to \tilde{\mathbf{Y}}_j)$ for all possible i, j. Hence, the bit error probability at the destination is given by

$$\begin{aligned} P_b &\leq \rho \sum_i \sum_{j,j\neq i} d_{ij} P_e(\tilde{\mathbf{Y}}_i \to \tilde{\mathbf{Y}}_j) \\ &\leq \rho \sum_i \sum_{j,j\neq i} d_{ij} \sum_{s_l\in\mathcal{S}} \left[\prod_{m=1}^{r_{sd}} \left(\frac{1}{1+\frac{\lambda_{sd}^{mij}\gamma_{sd}}{4P_{sd}}} \right)^{n_d} \right. \\ &\prod_{k\in\xi} \prod_{m=1}^{r_{r_kd}} \left(\frac{1}{1+\frac{\lambda_{r_kd}^{mij}\gamma_{r_kd}}{4P_{r_kd}}} \right)^{n_d} \\ &\left. \prod_{k\in\bar{\xi}} \left\{ \rho \sum_p \sum_{q,q\neq p} d_{pq} \prod_{m=1}^{r_{sr_k}} \left(\frac{1}{1+\frac{\lambda_{sr_k}^{mpq}\gamma_{sr_k}}{4P_{sr_k}}} \right)^{n_r} \right\} \right], \quad (26) \end{aligned}$$

where $d_{ij} = d_H(\bar{\mathbf{y}}_i, \bar{\mathbf{y}}_j)$ and $\bar{\xi}$ denotes the complement of ξ. At high SNRs, the additive unity term can be ignored in the denominator of (20). So, $P(\mathbf{a}=\mathbf{s}_l)$ can be approximated as

$$\begin{aligned} P(\mathbf{a}=\mathbf{s}_l) &\leq \prod_{k\in\bar{\xi}_l} \left\{ \rho \sum_p \sum_{q,q\neq p} d_{pq} \prod_{m=1}^{r_{sr_k}} \left(\frac{1}{\frac{\lambda_{sr_k}^{mpq}\gamma_{sr_k}}{4P_{sr_k}}} \right)^{n_r} \right\} \\ &= \prod_{k\in\bar{\xi}_l} \gamma_{sr_k}^{-n_r r_{sr_k}} \prod_{k\in\bar{\xi}_l} C_k, \quad (27) \end{aligned}$$

where $C_k = \rho\sum_p\sum_{q,q\neq p} d_{pq} \prod_{m=1}^{r_{sr_k}} \left(\frac{\lambda_{sr_k}^{mpq}}{4P_{sr_k}}\right)^{-n_r}$. Similarly $P_e(\tilde{\mathbf{Y}}_i \to \tilde{\mathbf{Y}}_j|\mathbf{a}=\mathbf{s}_l)$ can be written as

$$\begin{aligned} P_e(\tilde{\mathbf{Y}}_i \to \tilde{\mathbf{Y}}_j|\mathbf{a}=\mathbf{s}_l) &\leq \gamma_{sd}^{-n_d r_{sd}} \prod_{m=1}^{r_{sd}} \left(\frac{1}{\frac{\lambda_{sd}^{mij}}{4P_{sd}}} \right)^{n_d} \\ &\prod_{k\in\xi_l} (\gamma_{r_kd}^{-n_d r_{r_kd}}) \prod_{k\in\xi_l} \prod_{m=1}^{r_{r_kd}} \left(\frac{1}{\frac{\lambda_{r_kd}^{mij}}{4P_{r_kd}}} \right)^{n_d} \\ &= \gamma_{sd}^{-n_d r_{sd}} D_{ij} \prod_{k\in\xi_l} (\gamma_{r_kd}^{-n_d r_{r_kd}}) \prod_{k\in\xi_l} C_k^{ij}, \quad (28) \end{aligned}$$

where $D_{ij} = \prod_{m=1}^{r_{sd}} \left(\frac{\lambda_{sd}^{mij}}{4P_{sd}}\right)^{-n_d}$ and $C_k^{ij} = \prod_{m=1}^{r_{r_kd}} \left(\frac{\lambda_{r_kd}^{mij}}{4P_{r_kd}}\right)^{-n_d}$. Now, $P_e(\tilde{\mathbf{Y}}_i \to \tilde{\mathbf{Y}}_j)$ can be written as

$$\begin{aligned} P_e(\tilde{\mathbf{Y}}_i \to \tilde{\mathbf{Y}}_j) &\leq \sum_{\mathbf{s}_l\in\mathcal{S}} \prod_{k\in\bar{\xi}_l} \gamma_{sr_k}^{-n_r r_{sr_k}} \prod_{k\in\bar{\xi}_l} C_k \gamma_{sd}^{-n_d r_{sd}} D_{ij} \\ &\prod_{k\in\xi_l} \gamma_{r_kd}^{-n_d r_{r_kd}} \prod_{k\in\xi_l} C_k^{ij}. \quad (29) \end{aligned}$$

The vector $\mathbf{s}_l$ is a K-tuple vector. By convention, we can assign the first element of $\mathbf{s}_l$ for the state of the first relay, second element to the state of second relay, and so on. Therefore, (29) can be expanded as [12]

$$\begin{aligned} P_e(\tilde{\mathbf{Y}}_i \to \tilde{\mathbf{Y}}_j) &\leq \gamma_{sd}^{-n_d r_{sd}} D_{ij} [\gamma_{r_1d}^{-n_d r_{r_1d}} C_1^{ij} + \gamma_{sr_1}^{-n_r r_{sr_1}} C_1] \\ &\sum_{\mathbf{s}_l'\in\mathcal{S}'} \prod_{k\in\bar{\xi}_l, k\neq 1} \gamma_{sr_k}^{-n_r r_{sr_k}} \prod_{k\in\bar{\xi}_l, k\neq 1} C_k \\ &\prod_{k\in\xi_l, k\neq 1} \gamma_{r_kd}^{-n_d r_{r_kd}} \prod_{k\in\xi_l, k\neq 1} C_k^{ij}, \quad (30) \end{aligned}$$

where $\mathbf{s}_l'$ is the state vector except for the first relay and $\mathcal{S}'$ is the set of all possible states for the $K-1$ relays. In a similar way, we can expand for the remaining relays to get (21).

REFERENCES

[1] R. Hadani *et al.,* "Orthogonal time frequency space modulation," *Proc. IEEE WCNC'2017*, pp. 1-7, Mar. 2017.

[2] Y. Hong, T. Thaj, and E. Viterbo, *Delay-Doppler Communications: Principles and Applications*, Academic Press, 2022.

[3] P. Raviteja, K. T. Phan, Y. Hong, and E. Viterbo, "Interference cancellation and iterative detection for orthogonal time frequency space modulation," *IEEE Trans. Wireless Commun.*, vol. 17, no. 10, pp. 6501-6515, Aug. 2018.

[4] H. Qu, G. Liu, L. Zhang, S. Wen, and M. A. Imran, "Low-complexity symbol detection and interference cancellation for OTFS system," *IEEE Trans. Commun.*, vol. 69 no. 3, pp. 1524 - 1537, Dec. 2020.

[5] G. D. Surabhi, R. M. Augustine, and A. Chockalingam, "On the diversity of uncoded OTFS modulation in doubly-dispersive channels," *IEEE Trans. Wireless Commun.*, vol. 18, no. 6, pp. 3049-3063, Jun. 2019.

[6] V. S. Bhat, G. D. Surabhi, and A. Chockalingam, "Performance analysis of OTFS modulation with receive antenna selection," *IEEE Trans. Veh. Tech.*, vol. 70, no. 4, pp. 3382-3395, Apr. 2021.

[7] S. Li, J. Yuan, W. Yuan, Z. Wei, B. Bai, and D. W. K. Ng, "Performance analysis of coded OTFS systems over high-mobility channels," *IEEE Trans. Wireless Commun.*, vol. 20, no. 9, pp. 6033-6048, Sep. 2021.

[8] P. Singh, K. Yadav, H. B. Mishra, and R. Budhiraja, "BER analysis for OTFS zero forcing receiver," *IEEE Trans. Commun.*, vol. 70, no. 4, pp. 2281-2297, Apr. 2022.

[9] J. N. Laneman, D. N. C. Tse, and G. W. Wornell, "Cooperative diversity in wireless networks: Efficient protocols and outage behavior," *IEEE Trans. Inform. Theory*, vol. 50, no. 12, pp. 3062-3080, Dec. 2004.

[10] A. Nosratinia, T. E. Hunter, and A. Hedayat, "Cooperative communication in wireless networks," *IEEE Commun. Mag.*, vol. 42, no. 10, pp. 74-80, Oct. 2004.

[11] N. Varshney, A. V. Krishna, and A. K. Jagannatham, "Selective DF protocol for MIMO STBC based single/multiple relay cooperative communication: end-to-end performance and optimal power allocation," *IEEE Trans. Commun.*, vol. 63, no. 7, pp. 2458-2474, Jul. 2015.

[12] M. M. Fareed, M. Uysal, and T. A. Tsiftsis, "Error-rate performance analysis of cooperative OFDMA system with decode-and-forward relaying," *IEEE Trans. Veh. Tech.*, vol. 63, no. 5, pp. 2216-2223, Jun. 2014.

[13] Y. Khattabi and M. M. Matalgah, "Conventional and best-relay-selection cooperative protocols under nodes-mobility and imperfect-CSI impacts: BER performance," *Proc. IEEE WCNC'2015*, pp. 105-110, May 2015.

[14] A. M. S. Abdelgader and W. Lenan, "The physical layer of the IEEE 802.11p WAVE communication standard: the specifications and challenges," *Proc. World Congr. Eng. Comput. Sci.*, pp. 22-24, Oct. 2014.